AGU PUBLICATIONS

Global Biogeochemical Cycles

RESEARCH ARTICLE
10.1002/2015GB005275

Key Points:
- Hg speciation was determined along the 40°S parallel
- Hg(0) concentration differed in water masses and evaded from surface to atmosphere
- Organomercury compounds were associated with regions of lower oxygen or chlorophyll a peak

Correspondence to:
A. Bratkič,
arne.bratkic@vub.ac.be

Citation:
Bratkič, A., M. Vahčič, J. Kotnik, K., Obu Vazner, E., Begu, E. M. S. Woodward, and M. Horvat (2016), Mercury presence and speciation in the South Atlantic Ocean along the 40°S transect, *Global Biogeochem. Cycles*, *30*, 105–119, doi:10.1002/2015GB005275.

Received 26 AUG 2015
Accepted 5 JAN 2016
Accepted article online 7 JAN 2016
Published online 1 FEB 2016

Mercury presence and speciation in the South Atlantic Ocean along the 40°S transect

Arne Bratkič[1], Mitja Vahčič[1], Jože Kotnik[1], Kristina Obu Vazner[2,3], Ermira Begu[1,2], E. Malcolm S. Woodward[4], and Milena Horvat[1,2]

[1]Department of Environmental Sciences, Jožef Stefan Institute, Ljubljana, Slovenia, [2]International Postgraduate School Jožef Stefan, Jamova cesta 39, Ljubljana, Slovenia, [3]IEI, Institute for Ecological Engineering d.o.o., Maribor, Slovenia, [4]Plymouth Marine Laboratory, Plymouth, UK

Abstract Mercury (Hg) natural biogeochemical cycle is complex and a significant portion of biological and chemical transformation occurs in the marine environment. To better understand the presence and abundance of Hg species in the remote ocean regions, waters of South Atlantic Ocean along 40°S parallel were investigated during UK-GEOTRACES cruise GA10. Total mercury (THg), methylated mercury (MeHg), and dissolved gaseous mercury (DGM) concentrations were determined. The concentrations were very low in the range of pg/L (femtomolar). All Hg species had higher concentration in western than in eastern basin. THg did not appear to be a useful geotracer. Elevated methylated Hg species were commonly associated with low-oxygen water masses and occasionally with peaks of chlorophyll *a*, both involved with carbon (re)cycling. The overall highest MeHg concentrations were observed in the mixed layer (500 m) and in the vicinity of the Gough Island. Conversely, DGM concentrations showed distinct layering and differed between the water masses in a nutrient-like manner. DGM was lowest at surface, indicating degassing to the atmosphere, and was highest in the Upper Circumpolar Deep Water, where the oxygen concentration was lowest. DGM increased also in Antarctic Bottom Water. At one station, dimethylmercury was determined and showed increase in region with lowest oxygen saturation. Altogether, our data indicate that the South Atlantic Ocean could be a source of Hg to the atmosphere and that its biogeochemical transformations depend primarily upon carbon cycling and are thereby additionally prone to global ocean change.

1. Introduction

Mercury (Hg) is a potent harmful trace metal that does not have any beneficial biological function, but instead causes various ill effects in biota on all trophic levels [*United Nations Environment Programme (UNEP)*, 2013]. Hg occurrence in the environment has approximately tripled over time, mainly due to anthropogenic use of its deposits, burning of fossil fuels, and other industrial activities [*UNEP*, 2013; *Amos et al*., 2014]. Hg is present in all environmental compartments, with a large amount of that present in the world's Ocean, where is found in generally low concentrations [*Cossa et al*., 2011; *Mason et al*., 2012; *Lamborg et al*., 2014]. The ocean-borne fraction is particularly important as the seawater environments frequently serve as net producers of organic Hg species, these being highly bioenhancing and bioaccumulative, with significant deteriorating ecosystem and human health impact [*UNEP*, 2013; *Mason et al*., 2012]. All Hg species share a common precursor, Hg(II) ion, which is usually complexed with organic or inorganic ligands and is rarely truly dissolved in water. Together with gaseous elemental mercury (Hg(0)), they form an inorganic species pool in the oceans. Monomethylmercury (MeHg) and dimethylmercury (DMeHg) are both organic species, the former being usually complexed with a range of dissolved substances such as dissolved organic matter, and the latter being a dissolved gas [*Fitzgerald et al*., 2007].

As a consequence of the historical intense industrialization of Europe and North America, Hg increases have been observed in both the North Atlantic and North Pacific Oceans [*Sunderland et al*., 2009; *Mason et al*., 2012; *Lamborg et al*., 2014]. This increase was estimated to be 2–3 times the concentration of 100 years ago in the upper 100 m of the open ocean. The intermediate waters are reported to have increased by 25% and deep oceans by 11%, when compared to 100 years ago [*UNEP*, 2013]. This trend continues today as a consequence of industrialization of newly developing countries, but the estimates of these increases do not always agree [*UNEP*, 2013; *Kocman et al*., 2013; *Amos et al*., 2014; *Lamborg et al*., 2014]. Despite the fact that Western countries have reduced their Hg emissions, particularly to the atmosphere, the re-emission of historically

deposited Hg needs to be considered as an important part of contemporaneous emissions, as well as take into account new emissions from developing economies in the East [*Kocman et al.*, 2013; *Amos et al.*, 2014]. Fluxes of Hg species may often not be distinguished by their (re)emission origin. Being of particular importance for the oceans are wet and dry atmospheric deposition, and the resuspension of Hg buried in the sediments, which frequently occurs in the industrially or touristic developed coastal areas or in the deep sediments during offshore drilling operations and transoceanic seabed cable laying [*Amos et al.*, 2014]. Natural sources such as underwater volcanoes or from mid-ocean ridges are thought to be of minor global importance [*Mason et al.*, 2012].

The penetration of Hg into the oceans is correlated with the proximity to anthropogenic sources, input modes of Hg (i.e., rivers, runoff, and atmospheric deposition), and also the specific chemical form, all affecting its mobility. Although coastal areas are under considerably higher Hg stress, Hg export to open ocean areas is not negligible [*Amos et al.*, 2014]. Within the Ocean, Hg is transported between various water masses [*UNEP*, 2013], most important being vertical transport and downward particle scavenging, which is intimately connected with the biological pump [*Azam and Malfatti*, 2007; *Herndl and Rheinthaler*, 2013]. Simultaneously, Hg is also being transformed primarily by microbes between previously mentioned chemical species [*Barkay and Wagner-Döbler*, 2005]. Because Hg is strongly adsorptive, it binds onto particles of organic matter, which are usually hot spots of microbial activity. This phenomenon is therefore conducive for linking Hg biotransformations to oceanic primary production and the microbial carbon pump. The link between the two cycles is further intertwined with cycling of other major nutrients, such as oxygen, nitrogen, and iron. There is a profound difference between the upper mixed (photic) layer, where the biotic and photochemical components exert significant influence on short-term transformations of nutrients, and the deep ocean, which is characterized by slow changes in environmental conditions, suggestive of past and long-term transformations. As such, in the state of a globally changing ocean, Hg biogeotransformations need to be understood as the interplay of biological factors and variations in environmental conditions.

Remote areas, such as South Atlantic Ocean, receive Hg principally through aerial deposition, since the sedimentary and geothermal sources are thought to be only locally important, and fluvial discharges have limited influence [*Cossa et al.*, 2004; *Mason et al.*, 2012; *Amos et al.*, 2014]. Atmospheric Hg deposition to the global ocean surface is estimated at 3700 t/yr, mostly in the Hg(II) form [*UNEP*, 2013], and since the South Atlantic represents about 11% of the world's Ocean, this suggests that this area receives roughly 410 t of Hg per year by wet and dry deposition only. However, most of the deposited Hg (approximately 70%) is quickly re-emitted as Hg(0).

Nonetheless, water masses that are present at 40°S may be labeled by past Hg releases. For instance, North Atlantic Deep Water (NADW), which forms in the North Atlantic by the mixing and sinking of several water masses, did not have any contact with the surface for at least the past 300 years [*Thurman*, 1997]; therefore, it may carry information of European anthropogenic use of Hg from 1700 and later [*Cossa et al.*, 2011]. Additionally, subsurface eddies, large rotating lenses of Eurafrican Mediterranean Water coming into the Atlantic Ocean through the Strait of Gibraltar with a higher natural Hg content, are introduced into the NADW [*Tomczak and Godfrey*, 1994]. Similarly, newly formed Antarctic Bottom Water (AABW) and Antarctic Intermediate Water (AAIW) can be Hg-characterized by sea ice formation or thawing [*Cossa et al.*, 2011; *Fisher et al.*, 2012]. Upper Circumpolar Deep Water (UCDW) Hg content may be more difficult to interpret since this water mass is created by mixing of the aforementioned water masses. UCDW has been slowly traveling at depth in the Indian and Pacific Oceans, consuming oxygen from organic matter (OM) degradation, and consequently altering its redox state, which is very important in terms of controlling environmental Hg speciation, stability, and bioavailability [*Barkay et al.*, 2003].

The investigated South Atlantic 40°S transect passes through part of the South Subtropical Convergence (SSTC), which is characterized by changing surface nutrient regimes, and is effectively borderline between macronutrient-limited, Fe-replete South Atlantic Gyre water, and the macronutrient-rich, Fe-depleted Antarctic Circumpolar Current (ACC) [*Browning et al.*, 2014]. The potential for Hg biogeochemical transformations in this region is therefore high. The variable conditions, which affect microbial and phytoplankton communities in this area, are thus expected to exert significant influence also on Hg biogeotransformations. Nutrient regimes and Fe availability in particular, having strong control over phytoplankton primary production and physiology in the South Atlantic, will therefore also be of primary concern for Hg speciation in the upper mixed layer [*Browning et al.*, 2014]. The intermediate depths and deep waters are expected to be influenced by the biological pump and sinking organic matter, as well as physico-chemical parameters of the dark ocean [*Azam and Malfatti*, 2007; *Herndl and Rheinthaler*, 2013; *Mason et al.*, 2012].

This study was primarily focused on delivering high-quality, spatially high-resolution data, as well as contributing to the existing Hg speciation data in remote ocean environments. Speciation data, presented here, are a small step toward elucidating the prevalent Hg biogeotransformations in differing water masses according to their nutrient, biological, and other physico-chemical status, thus serving as a link between past Hg ocean changes and future predictions. The sampling, dissolved gaseous mercury (DGM), and THg measurements were performed onboard *RRS* James Cook, between December 2011 and January 2012 during cruise JC068. The cruise was part of UK-GEOTRACES program (cruise GA10). The mercury investigation was also part of Global Mercury Observation System (GMOS) project.

2. Materials and Methods

2.1. Chemicals

Deionized water from an onboard Milli-Q system (18.2 MΩ: Millipore, Bedford, MA, USA) was used for rinsing and cleaning of all glassware. Thirty percent hydrochloric acid (HCl) (Suprapure, Merck®, Darmstadt, Germany) was used for pH adjustment and preservation of all seawater samples. Bromine chloride (BrCl) used for oxidation of all Hg species in seawater samples was prepared from KBrO3 (EMSURE®, Merck, Darmstadt, Germany), KBr (EMSURE®, Merck, Darmstadt, Germany), Milli-Q, and HCl (EMSURE®, Merck, Darmstadt, Germany). Twelve percent solution of hydroxylamine hydrochloride ($NH_2OH \cdot HCl$) used for removal of BrCl was prepared from $NH_2OH \cdot HCl$ (EMSURE®, Merck, Darmstadt, Germany) salt, and Milli-Q water. Tin chloride ($SnCl_2$) solution used for reduction of Hg species was prepared from tin(II) chloride dehydrate ($SnCl_2$*$2H_2O$), 98% sulphuric acid (H_2SO_4) (EMSURE®, Merck, Darmstadt, Germany), and Milli-Q water. A 100 ng/mL Hg(II) standard solution used for total Hg calibration was prepared from 1000 mg/mL (Certipur®, Merck, Darmstadt, Germany) $Hg(NO_3)_2$ certified standard solution, traceable to National Institute of Standards and Technology Standard Reference Material by serial dilutions.

2.2. Materials

Tenax (Tenax TA, 20/35 mesh Alltech, Deerfield, IL, USA) traps were used for collection of dimethyl mercury (DMeHg) and methyl mercury (MeHg). Gold-coated sand traps used in the double amalgamation system were obtained from Tekran (Tekran Instruments Corporation, Toronto, Canada). For calibration of the cold vapor atomic fluorescence spectroscopy (CVAFS) Hg detector 50 and 100 μL gas tight syringes (1800 Series Gastight syringe, Hamilton®, Nevada, USA) were used. For sample storage, transportation, and onboard analysis, 0.5 L and 0.2 L acid-cleaned Teflon bottles were used. For onboard DGM and DMeHg purging, quartz 0.5 L and 2 L glass bubblers were used.

2.3. Instruments

For onboard DGM, DmeHg, and total mercury analyses a Brooks Rand® Model III CVAF detector was used, and for its calibration a Tekran, Model 2505, mercury vapor calibration unit was used. For MeHg determination in the home laboratory a distillation heating block (Tekran model 2750) was used for extraction of MeHg from ocean water samples and a Brooks Rand MERX® system for MeHg detection.

2.4. Gases

For DGM and total Hg purging from seawater mercury- and oxygen-free nitrogen (N_2) gas was used (BOC Group plc). For the CVAFS double amalgamation system Hg-free argon gas was used (Ar) (BOC Group plc).

2.5. Sampling

Water samples were collected with both stainless steel (SS) and titanium (Ti) conductivity-temperature-depth (CTD)/rosette sampling systems. The SS rosette was equipped with 24 × 20 L Niskin sampling bottles and the Ti rosette with 24 × 10 L Teflon coated sampling bottles equipped with Teflon O-rings and valves. The Ti system was deployed on a conducting Kevlar cable to reduce the possibility of contamination through leaching. The SS rosette was also equipped with a CTD (Seabird SBE 911+) probe (salinity, temperature, and depth), a chlorophyll *a* spectrophotometric sensor (Chelsea Aquatracka MKIII fluorometer), and an oxygen concentration probe (Seabird SBE 43).

2.6. Nutrients

Nutrients were determined on board following the methods described by *Woodward and Rees* [2001] and using Bran and Lube AAIII segmented flow colorimetric analyzer. No samples were frozen or stored and were all analyzed within 1 h of sampling [*Hydes et al*., 2010].

2.7. Hg Speciation

Ocean water samples for postcruise THg and MeHg laboratory analyses were collected into acid precleaned 0.5 L Teflon bottles from the Ti rosette. Prior to the sampling, bottles were rinsed 3 times with the ocean water from the Niskin sampling bottle, filled with the sample and then acidified with 30% HCl to adjust the pH to 1. Closed bottles were then packed into two zip-lock bags and frozen at −20°C during the entire length of the voyage, and then subsequently during the transport to the laboratory, where total Hg and MeHg were determined.

Samples for onboard DGM determination were collected from the Niskin bottles (SS rosette) immediately after the collection of ^{3}He, dissolved inorganic carbon, and nutrient samples. The samples were transferred directly into 0.5 L glass bubblers using silicone tubing to prevent degassing of volatile Hg species, and to avoid contamination. Volatile species were purged from the sample onto a gold-coated sand trap using a bubble stream of Hg-free nitrogen gas for 10 min. The trap was then removed from the bubbler and analyzed on a double amalgamation CVAFS system [*Horvat et al*., 2003; *Gårdfeldt et al*., 2003; *Kotnik et al*., 2007]. The detection limit of the method used was 4 pg/L, which was calculated from three standard deviations of the blank. The repeatability of the method was 4% and was determined by measuring 10 consecutive replicate samples at the same concentration.

Samples for the onboard THg determination were transferred into 0.2 L Teflon bottles from the SS rosette, acidified with HCl acid, spiked with BrCl, and irradiated in an UV light chamber for at least 3 h to facilitate the oxidation of Hg species before the reduction and the subsequent analysis of total Hg on a double amalgamation CVAFS detection system ([*Horvat et al*., 2003] U.S. Environmental Protection Agency (EPA) method 1631). To monitor the stability of the measurement system, a calibration curve (0, 25, 50, and 100 pg/L] was determined at the beginning and the end of each measuring sequence, with 50 ng/mL solutions measured after every four samples. The length of day (LOD) of the method was calculated at 0.2 pg/L and was based on 3 standard deviations of the reagent blank sample.

MeHg in the samples was determined after a distillation process [*Horvat et al*., 1993]. It should be noted that the MeHg results reported in this work signify the sum of both MeHg and DMeHg, except at Station 20 where DMeHg was determined separately and its values subtracted from MeHg values. In addition, note that all MeHg concentrations are reported as pg of Hg, rather than as MeHg.

For distillation, approximately 50 g of a water sample was weighed directly in a 60 mL screw capped Teflon vial [*Horvat et al*., 1993]; the vial was then closed and put into the distillation unit at a heating-block temperature of 122°C. The distillate was collected in a 40 mL measuring glass vial, and the distillation continued until at least 40 g of distillate was collected. The pH was then adjusted to 4.6 by addition of 300 μL of acetate buffer. Fifty microliters of 1% $NaBEt_4$ was added to the measuring vial; the vial was filled with Milli-Q water, capped, and placed in a Brooks Rand MERX® system (U.S. EPA method 1630). The purging time was set to 5 min. Ethylated MeHg, as ethylmethylmercury, was purged onto a Tenax trap and then thermally desorbed (180°C) onto an isothermal GC column (OV-3). Hg species were converted to Hg(0) by pyrolysis at 600°C and measured by a cold vapor atomic fluorescence detector (CVAFS) [*Liang et al*., 1994]. Spike recovery was made for each batch of analyses and ranged from 75% to 95%. The results were then corrected for the recovery factors obtained for each batch. The LOD was calculated based on three times the standard deviation of the reagent blanks and varied between 6 pg/L and 23 pg/L.

DMeHg samples were collected only at sampling Station 19 (50.58°W, 38.05°S) (Figure 1). Two liters of ocean water was transferred into a glass bubbler using silicone tubing to prevent degassing. A Tenax trap was attached to the filled bubbler, which was then purged with Hg-free nitrogen gas at 300 mL/min for 10 min. After that, the traps were removed from the bubbler, closed on both sides with Teflon plugs, and then sealed inside double plastic bags from which the air was evacuated. These were then frozen at −20°C and stored at that temperature for the entire length of the voyage and subsequent transport back to the laboratory, where DMeHg was determined [*Bloom and Fitzgerald*, 1988]. Briefly, the GC column was immersed in liquid nitrogen

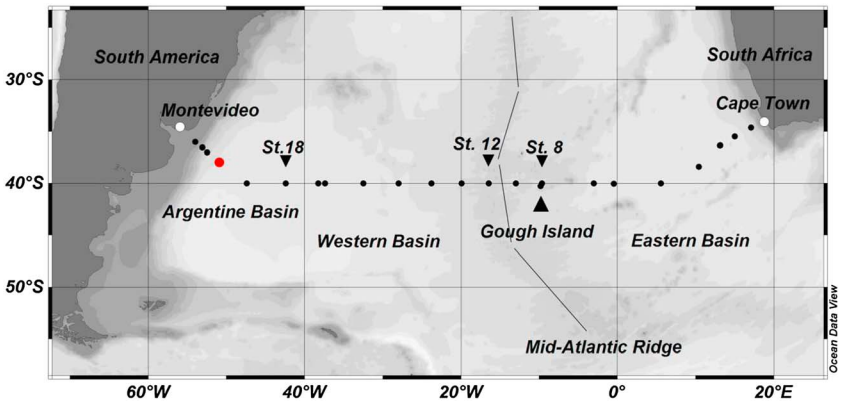

Figure 1. Representation of the stations occupied during GA10 GEOTRACES cruise from 24 December 2011 to 27 January 2012. Ship sailed from Cape Town, South Africa, and landed in Montevideo, Uruguay (white dots). Red dot represents Station 20, which was devoted to Hg speciation sampling and was the only station where DMeHg was determined. Black triangle points to location of Gough Island (Station 9) (40.32°S 9.94°W), with THg and MeHg increases. Black lines indicate the approximate position of the Mid-Atlantic Ridge central axis. See text for discussion on Stations 8, 12, and 18, marked by inverted black triangles.

for 3 min and flushed with argon for an additional 3 min. Then, the Tenax trap was connected to the GC column and heated at 200°C for 7 min. After heating, the trap was disconnected and the GC column was transferred to a heated oven (180°C). Under a flow of argon gas the eluted Hg species were converted into Hg(0) by pyrolytic decomposition at 600°C, and then measured on a CVAFS detector. The LOD, based on 3 standard deviations of the baseline noise, was estimated to be 0.2 pg/L.

3. Results and Discussion

3.1. General Hydrographical Settings and Nutrient Status

Water masses, distinguished by oxygen content, salinity, temperature, and the major nutrients in the investigated region during the 40°S transect (Figure 1) voyage are shown in Figure 2. The voyage crossed the SSTC (~16°C surface temperature) in the eastern basin and approximately midway in distance between the two continents. The SSTC is known to migrate northward and southward in relation to changes in flow rates of Agulhas Current, which also affects the South Atlantic Gyre size [*Browning et al*., 2014]. Variations in temperature, salinity, and some nutrients (N, P, and Si) on the continental margins correspond to the intrusion of the Agulhas Current from Indian Ocean on the African side, and Rio de la Plata discharge on the South American side (Figures 1 and 2). These are therefore additional entry points for the dilution or addition of Hg into the waters of the South Atlantic, being separate from atmospheric depositions. The intermediate and deep waters of the 40°S parallel below the mixed layer (~500 m) are (from top down) Antarctic Intermediate Water (AAIW), Upper Circumpolar Deep Water (UCDW), North Atlantic Deep Water (NADW), and Antarctic Bottom Water (AABW) and are distinguished by the above-mentioned properties (Figure 2). The Mid-Atlantic Ridge (MAR) divides the South Atlantic Ocean into two basins, whose deep waters do not readily mix horizontally although they share a common origin through vertical sinking of waters along Antarctic shelf in the Weddell Sea [*Thurman*, 1997; *Wyatt et al*., 2014]. Nevertheless, this division is not apparent in any nutrient or physico-chemical distributions (Figure 2).

3.2. THg Distribution

Total mercury concentrations were 0.29 ± 0.12 ng/L and are similar to previous measurements in the Atlantic and other oceans [*Mason et al*., 1998, 2012; *Bowman et al*., 2015]. THg distributions in the water column in this region did not appear to be useful in tracing water masses—the Hg content of any water mass is not different from the other and no horizontal layering was noticed (Figure 3). The decoupling of THg dynamics from profiles of temperature, salinity, or nutrients suggests that overall Hg distribution is not controlled simply by these factors. This is not surprising, since Hg exhibits strong adsorptive properties and is generally distributed according to presence and concentration of organic matter (OM), which has usually slow sedimentation flux. Long residence time of THg in the water column therefore leads to uniform mixing,

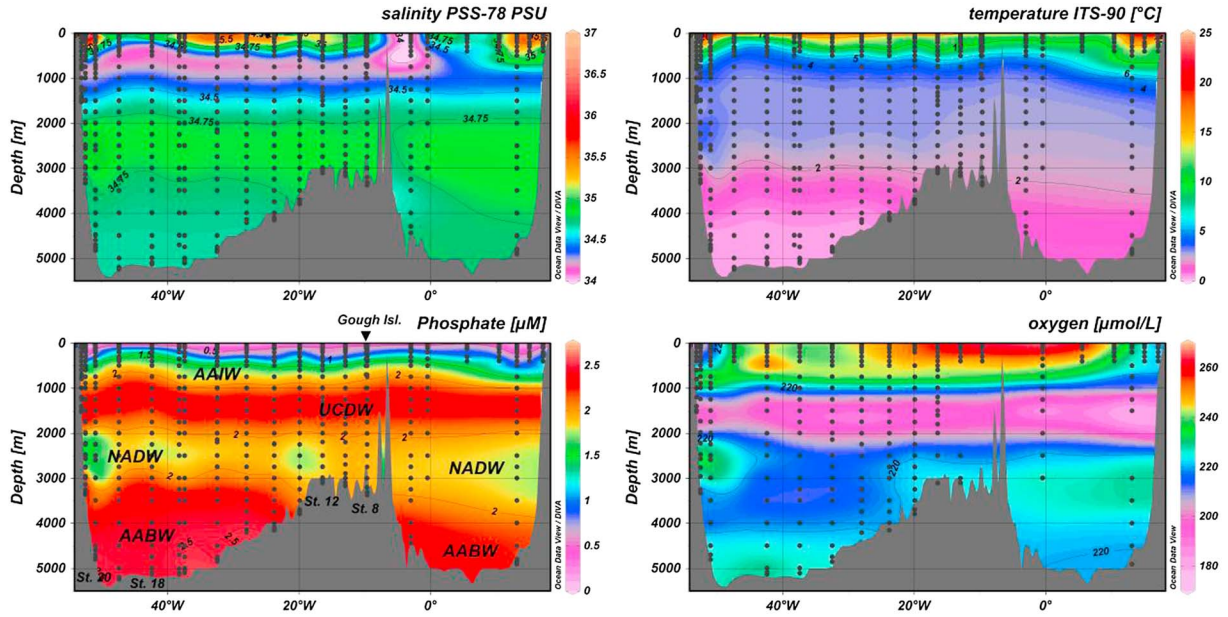

Figure 2. Salinity, temperature, phosphate, and oxygen profiles for GA10 cruise along 40°S parallel. Water masses can be distinguished by various parameters, most evidently by salinity and phosphate profiles. Grey dots show the sampling depths. Phosphate figure also indicates abbreviations for water masses: Antarctic Intermediate Water (AAIW), Upper Circumpolar Deep water (UCDW), North Atlantic Deep Water (NADW), and Antarctic Bottom Water (AABW).

which is reflected in our profiles [*Amos et al*., 2014; *Zhang et al*., 2014; *Bowman et al*., 2015]. We have also not observed the nutrient-like distribution of THg and its correlation with phosphate as was shown before [*Lamborg et al*., 2014]. Altogether, THg concentration could not be used as a tracer for water masses in the South Atlantic Ocean.

Despite this, some trends were observed in the concentration distribution, most notably that THg values in the western basin were 14% higher compared to those in eastern basin (0.29 ± 0.01 ng/L, 0.25 ± 0.01 ng/L, respectively, $p < 0.05$; Figure 3). It seems unlikely that the MAR could have influenced the entire western basin in the South Atlantic, although the plume from the ridge does turn westward and may carry its imprint. Possible influence by Mediterranean eddies could not be evaluated and is uncertain [*Tomczak and Godfrey*, 1994]. More probable is dry or wet atmospheric deposition, which is by far the most important source of Hg to this remote area, as well as preserved difference from North Atlantic [*Bowman et al*., 2015]. Ineffective scavenging of particle associated Hg may also play a role, as it can be recycled within the mixed layer for some time before settling [*Herndl and Rheinthaler*, 2013; *Mason et al*., 2012].

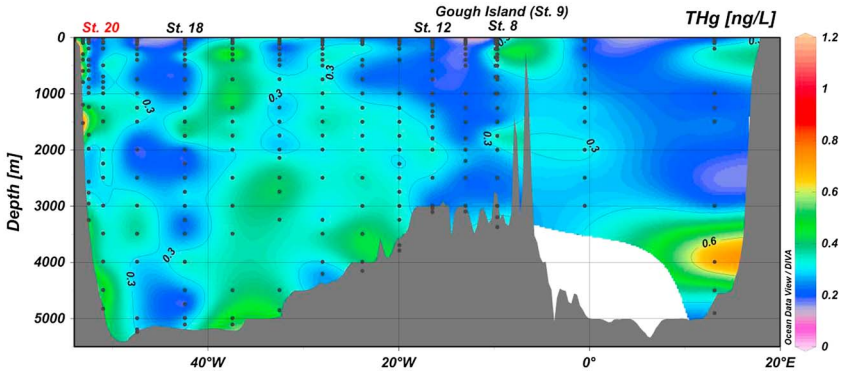

Figure 3. Full depth concentration profile of total Hg (THg) for GA10 transect. Grey dots indicate sampling depths. There was no apparent vertical stratification of THg relating to the water masses present at this latitude, suggesting that THg profiles are not to be very useful in tracing water masses. Nonetheless, it appears that THg is higher in concentrations in the western, compared to eastern basin.

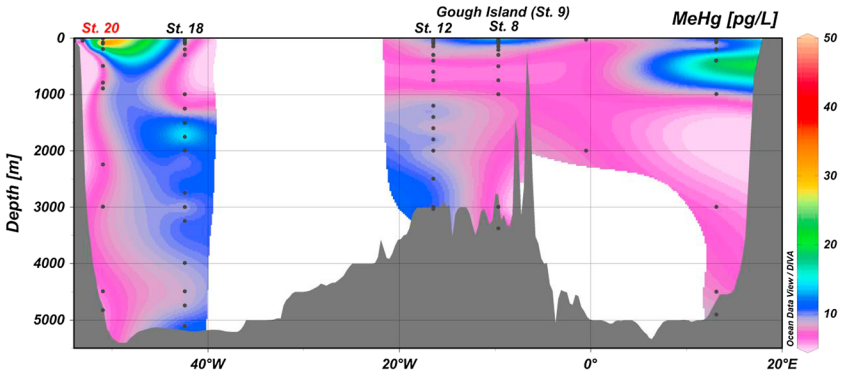

Figure 4. Depth profile for MeHg concentrations along the 40°S parallel. Grey dots indicate sampling depths. The values were generally very low and no strong variation was observed; however, the western basing shows slightly higher concentrations than eastern. Some MeHg appear to be of sedimentary origin, while the continental shelves do not seem to be important source to the water column. Sampling station at Gough Island at approximately 10°W, showed MeHg increase in the upper waters.

This is similar to results of *Bowman et al*. [2015], who have observed 15% higher west THg concentration in NADW in North Atlantic Ocean. NADW east of MAR in that region is older than the west NADW, and the difference was attributed to anthropogenic contribution in downwelled water during NADW formation [*Bowman et al*., 2015]. Our data for east and west NADW (Stations 1–11 and 12–24, respectively) were not statistically different ($p > 0.05$). It is possible that the aging of water masses, subjected to mixing, deposition, and scavenging, had obscured the signal, observed by *Bowman et al*. [2015]. Arguably, a more likely explanation is that anthropogenic contribution was insignificant when the present-day NADW in South Atlantic had been formed approximately 300 years ago [*Thurman*, 1997],

At the time of GA10 cruise the Copahue volcano was active at the Chile-Argentinean border in the Andes and was emitting soot and dust particles, which were transported eastward over the South Atlantic Ocean together with the Patagonian dust plume [*Johnson et al*., 2011]. Sea surface THg distribution, however, did not show elevated values neither in the eastern or western basin, where the particles are thought to have deposited (Figure 3). In fact, THg at the surface followed consistently the behavior of DGM and was generally depleted throughout the cruise, with some variation (Stations 8 and 17). It is possible that most of the Hg deposited was quickly re-emitted back to the atmosphere, the rest adsorbed onto available binding sites and sank quickly, or that Hg was ejected directly into the troposphere, undergoing a fast and long-range transport, eventually depositing remote from its source [*UNEP*, 2013].

There were also some discreet increases of THg along the continental slope on both sides of the ocean (Figure 3). These confirmed the fact that the continents and their oceanic borders can be a local source of Hg to the water column, but with limited influence [*Mason et al*., 2012]. These sources can be locally emphasized by continental slope phenomena such as turbidity currents or mud slides, transporting larger amounts of Hg further down toward the abyssal plain in a single event [*Thurman*, 1997]. Two increases were also observed near the seafloor, one in the eastern part of Argentine basin and the other above the MAR. The sediments are often a source of Hg to the water column, usually by diffusion, which can be emphasized by faunal resuspension or strong bottom currents. The increase at the MAR, however, was expected since geothermal sources are known for releasing Hg to the water column [*Lamborg et al*., 2006; *Mason et al*., 2012], albeit in lower amounts. The absence of strong THg increases above the MAR and the further increase in the water column suggests that most of the emitted Hg quickly precipitates upon mixing of hydrothermal vent fluids with ambient seawater [*Vetriani et al*., 2005]. As a consequence, only local Hg enrichment occurs, acting as a stressor on the indigenous microbial and faunal populations [*Vetriani et al*., 2005].

3.3. Methylated Mercury Species

Due to very low concentrations of MeHg and the volume of sample available for Hg determination, some of MeHg measurements fell below the limit of detection (Figure 4). Cruise-related longer storage of the samples (3 months) may have also contributed to overall low MeHg values. The storage and transport issues may adversely influence MeHg stability in the water sample during longer periods of time and may be to

some degree responsible for the variability of MeHg results observed [*Leopold et al*., 2010]. In addition, the procedures employed are not always the same by different authors, making exact comparisons sometimes difficult [*Cossa et al*., 2011; *Hammerschmidt and Bowman*, 2012; *Lamborg et al*., 2014; *Bowman et al*., 2015; and this study].

Nonetheless, the measurements indicate that the majority of MeHg was present in the mixed layer of the water column below the Chl *a* peak, confirming previous observations that MeHg formation is linked with organic matter degradation and subsequent release from OM during remineralization [*Heimbürger et al*., 2010; *Hammerschmidt and Bowman*, 2012; *Horvat et al*., 2003; *Lehnherr et al*., 2011; *Cossa et al*., 2011; *Zhang et al*., 2014; *Bowman et al*., 2015]. This is consistent with the idea that suspended or sinking particles of OM provide a safe environment for methylating microbes, coupling energy source, and Hg(II) [*Cossa et al*., 2011]. In addition, there is a possibility of oxygen depletion in these particles, where suboxic or anoxic methylation could take place, despite an otherwise oxygenated water column. It is also possible that part of the observed MeHg is actually the degradation product of DMeHg. There were also some individual increases in MeHg concentration, which are discussed below.

At two stations, 8 and 18 (Figure 4), MeHg peak was found at the same depth as Chl *a* peak. This indicates that there might be a portion of Hg methylation not linked only with OM degradation, or that some parts of new OM are rapidly recycled, or that phototrophy may be directly or indirectly involved in methylation process. Our current understanding of Hg methylation by phototrophic microbes is poor; however, the methylation can indirectly be linked with phototrophy through degradation of newly formed organic matter or through production of methylating metabolites [*Grégoire and Poulain*, 2014]. Direct phototrophic methylation has also been observed, but more research is needed in that area [*Pongratz and Heumann*, 1998]. Nevertheless, the fate of MeHg formed at Chl *a* peak is dubious; it could be either photodegraded or stable due to stabilisation by OM and because phototrophic organisms have so far not been found to contain *mer* operon [*Barkay et al*., 2010].

At sampling Station 9 (Gough Island), MeHg exhibited a general surface increase, an indication of local stimulating influence to MeHg formation, probably through an increase of the microbial respiration. That, in turn, is likely a consequence of Fe leaching into the water from island itself, which induces phytoplankton growth and subsequently OM remineralization. Gough Island indeed exhibits a strong influence over local microbial populations [*Browning et al*., 2014]. Moreover, islands generally stimulate species richness, and if they are simultaneously also bioreactors for MeHg production, this may suggest that an important part of MeHg content in certain fish species stems from localized source.

There were also two apparent increases in the concentration of MeHg near the surface, observed at both continental margins (Figure 4). The western increase could be explained by the mercury transport from the Rio de la Plata [*Ronco et al*., 2001], and the eastern increase may be a result of anthropogenic activities from South Africa, or alternatively, an intrusion of water from the Indian Ocean (Agulhas current). However, both sources would have primarily increased upper surface waters, yet the observed increase close to South African coast was at a depth of 500 m. Therefore, it may also be simply a signal of enhanced methylation stimulated by OM degradation at this particular depth.

The average value of MeHg in the upper 500 m of the water column was 11.3 pg/L. Assuming that this number represents a stable ratio between methylation, demethylation, and reduction processes, there is approximately 230 t of MeHg in the entire mixed layer of South Atlantic Ocean (which covers roughly 11.1% of the world's ocean surface, according to ETOPO1). Taking into account the bioaccumulative properties of MeHg, this amount of neurotoxin is ready to be incorporated into biomass since it is present in the area that is considered most biologically active in this region. Thus, external drivers (increasing temperature, organic matter content and availability, decreasing oxygen concentration, etc.), stimulating MeHg formation or prolonging its stability in the water column, which is about a year, have the possibility of considerably changing Hg species distribution and ratios between transformation processes [*Mason et al*., 2012]. Modeling approaches can be of use to describe future trends in biogeotransformations but are hindered by the variation in estimation of past released Hg and also by difficulty in predicting changes of future Hg sources [*UNEP*, 2013; *Kocman et al*., 2013; *Amos et al*., 2014; *Lamborg et al*., 2014].

It is interesting to note that MeHg (as well as THg and DGM, see discussion) values are uniformly lower in AAIW, compared to above- and below-lying waters. This indicates a depletion of MeHg in the surface waters,

which later become AAIW. It may also be speculated that the properties of AAIW do not support MeHg formation. If most of reducible Hg(II) is lost by reduction to the atmosphere in pre-AAIW surface water, this may be also simultaneous loss of methylable Hg and could help explain lower MeHg in the AAIW.

Despite scarcity of data, there appears an east-west difference in distribution of MeHg. The results (Figure 4) show that MeHg seems to be more abundant in the western basin, compared to eastern. This is similar to observed distribution in North Atlantic [*Bowman et al*., 2015]. MeHg life-time and age difference between waters of North and South Atlantic Ocean suggests that there is probably no common motive, explaining the observed trend. As most of the MeHg is formed in the layers of enhanced biological activity, scavenging is likely to be most important vector to the deep ocean. Speed of sinking material is size and weight dependent; therefore, the samples represent an integration of seasonally changing surface bioproduction, local deep ocean activity, advection, and mixing. This certainly bears on the whole how much the observed distributions between North and South Atlantic are related to one another.

The sediments are recognized as both an important source and depository of MeHg, especially in the coastal and shelf waters [*Mason et al*., 2006; *Monperrus et al*., 2007; *Merritt and Amirbahman*, 2009; *Emili et al*., 2011; *Bratkič et al*., 2013], but are not thought to be significant in terms of increasing concentrations in the open ocean [*Vetriani et al*., 2005; *Lamborg et al*., 2006; *Ogrinc et al*., 2007; *Mason et al*., 2012; *Amos et al*., 2014]. The Argentinean basin is an area of enhanced sedimentation, influenced also by transport of Rio de la Plata; therefore, it is expected that sediments may be a source of MeHg to the water column, as our results indicate. Interesting is also the relatively lower concentration of MeHg closer to the South American continental shelf (between Station 20 and Montevideo) compared to the open ocean, which further suggests that MeHg is not of geogenic origin. On the other hand, the observed increase in MeHg at the bottom above the MAR (Stations 8 and 12) was not expected, because hydrothermal fluids are not thought to be a significant source of MeHg to the ocean [*Lamborg et al*., 2006; *UNEP*, 2013]. Additionally, MeHg is not formed in all types of geothermal vents and strongly depends on the presence of organic matter at the seafloor through which the hydrothermal fluid passes. Most of the Hg (including possible MeHg) precipitates out of the hydrothermal fluid upon mixing with ambient seawater [*Vetriani et al*., 2005]. Also, the worldwide distribution of hydrothermal vents has not been determined in detail yet, which makes the assessment of hydrothermal influence more uncertain. All in all, it cannot be said with certainty that the observed increases were due to hydrothermal fluid discharge, and MeHg could have been formed by local microbiota, mobilizing precipitated HgS, and releasing MeHg to the water column. Altogether, THg and MeHg concentrations at the top of the MAR indicate that the hydrothermal phenomena associated with this oceanic spreading center are not basin-wide important sources of Hg to the South Atlantic, but more of a specific point source.

Station 20 was particularly intended for Hg measurements, especially for the determination of dimethylmercury (DMeHg). Its vertical distribution is shown in Figure 5. Clearly, DMeHg increases strongly below 1000 m in the UCDW, which exhibited overall lowest oxygen saturation. The exact process of DMeHg formation is unknown, but results indicate that it is produced primarily by microbes and is stable in deep ocean waters [*Baldi*, 1997; *Mason and Sullivan*, 1999; *Fitzgerald and Lamborg*, 2003; *Fitzgerald et al*., 2007; *Horvat et al*., 2003; *Kotnik et al*., 2007; *Cossa et al*., 2011; *Hammerschmidt and Bowman*, 2012]. Higher concentrations of DMeHg in UCDW and AABW did not resemble their respective oxygen concentration profile, suggesting that oxygen status of the water column is not simply governing DMeHg formation. On the other hand, UCDW has the highest nutrient concentrations due to bacterial degradation of OM during deep circulation in the Pacific and Indian Oceans, compared to other water masses, including NADW, AABW, and AAIW, which mix to form UCDW and Circumpolar Deep Water [*Emery*, 2001]. These converging gradients could represent the necessary environment for DMeHg formation.

3.4. Dissolved Gaseous Mercury

DGM concentrations displayed the largest variability and varied from 2 to 114 pg/L, with an average of 45 ± 29 pg/L (Figure 6). DGM also represented between 5 and 56 % of THg in investigated waters, with the ratio between DGM and THg being higher in the deep waters. Surface waters of the open ocean were depleted (approximately 10–15 pg/L), which was a consequence of the high volatility and low solubility of dissolved Hg(0) (Henry's constant 0.3 and 60 μg Hg(0)/L, respectively) [*Barkay et al*., 2003]. Average concentration of DGM above and below 500 m was 23 ± 16 pg/L and 73 ± 15 pg/L, respectively. That is, approximately 470 t in

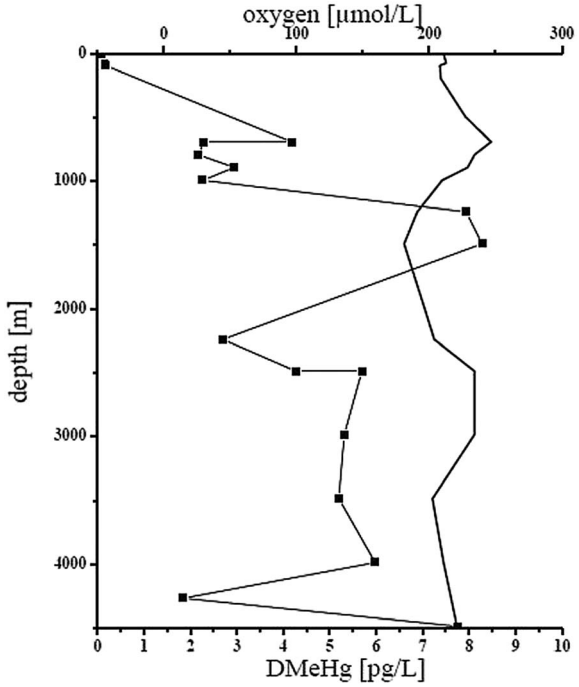

Figure 5. Vertical distribution of DMeHg (black squares line) and oxygen (plain line) at Station 20, dedicated for Hg measurements. DMeHg is a very volatile and unstable compound, present in very small quantities, which demand at least 2 L of sample. Very apparent is sudden increase of DMeHg in UCDW (around 1500 m) where oxygen concentration was lowest.

mixed layer and 10,200 t below that. Although mixed layer content is more susceptible to degassing to the atmosphere, a significant, though variable portion of the released Hg has been recently deposited to the ocean surface and is not originating from ocean interior [*Zhang et al.*, 2014]. Such evasion contributes significantly to the global budget of Hg(0) in the atmosphere [*Pirrone et al.*, 2010], but it is important to note that oceanic regions may change their role as sources or sinks of atmospheric Hg(0) seasonally [*Grégoire and Poulain*, 2014]. The interior of the ocean acts as a storage and biogeotransformation incubator for Hg, with consequences that will become a matter of atmospheric importance much later and elsewhere on the ocean's surface.

The stations sampled above the continental shelf regions (Figure 6) show a slight increase in DGM concentrations. At the South African side, the concentrations were elevated to 50 pg/L in the uppermost surface waters. This was possibly a signal from industrially intensive areas, such as Cape Town, yet might also be a signal from mixing waters of the Agulhas current, which were evident from temperature and salinity distribution (Figure 2) [*Donners et al.*, 2005]. On the South American side, elevated DGM values were likely associated with the intensive industrial and dense population characteristics of the estuary of Rio de la Plata, and the outfall from the cities and industrial regions of Buenos Aires and Montevideo. Mixing of salt and freshwater has been shown to increase DGM [*Bratkič et al.*, 2013], and in addition, the Rio de la Plata transports much sedimentary matter, which contains on average up to 0.5 Hg mg/kg [*Ronco et al.*, 2001]. As the environmental conditions change, particularly temperature, salinity, and redox potential, the bioavailability and reducibility of Hg change along with its partitioning between dissolved and solid phases [*Coquery and Cossa*, 1995; *Barkay et al.*, 1997; *Hines et al.*, 2006; *Emili et al.*, 2011].

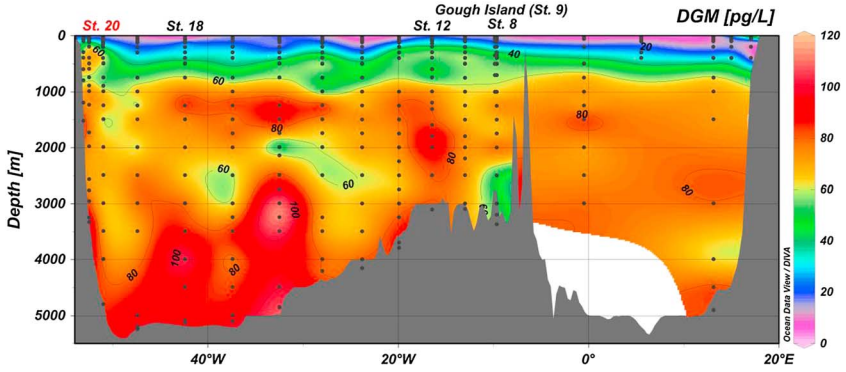

Figure 6. Full depth DGM distribution along the transect GA10. Grey dots indicate sampling depths. Horizontal layering is observable, following the general situation of water masses. UCDW showed on average higher DGM concentrations, sandwiched between AAIW and NADW. DGM concentrations increased downward, but were generally depleted at surface, evading into the atmosphere. AABW features highest DGM concentrations.

DGM distribution in the open ocean displayed a stratified structure, and several layers were distinguishable (Figure 6). Below the AAIW, with an average of 50 pg/L (~1000 t), UCDW DGM values increased around the 1500 m depth contour and averaged approximately 75 pg/L (~3020 t). NADW between 2000 m and 3000 m featured somewhat decreased (63 pg/L, ~2500 t), but also the most variable DGM concentrations, which again increased in the AABW (87 pg/L, ~3519 t), especially in the Argentine Basin. It is interesting to note that UCDW had higher DGM concentrations and DGM content. Given its history of OM decomposition and low oxygen concentration, it is probable that OM degradation leads to enhanced DGM production, which is preserved by lower O_2 values. In contrast, NADW had lower DGM, but THg did not significantly differ from neighbouring water masses. It appears therefore that biogeochemical reactions have not (yet) produced enough reducing equivalents that there is relatively less reducible Hg available or that slightly higher salinity content of NADW interferes with accumulation or formation of DGM.

Also, DGM increase was coincident with a THg increase in a westward direction from the MAR, toward South America. It is possible that Hg(0) could be transported over long distances in cold and dark ocean water, where oxidation and scavenging would be slower [*Mason et al*., 2012]. Nonetheless, the existing data [*Lamborg et al*., 2006; *Mason et al*., 2012; *Bowman et al*., 2015] suggest that hydrothermal vents most likely increase submarine environments only locally and precipitate as HgS upon mixing with surrounding seawater [*Vetriani et al*., 2005].

Higher concentrations of DGM (as well as THg) were also measured in the Argentine Basin, a more than 5000 m deep submarine formation with an abyssal plain. The AABW current, after being formed in the Weddel and Ross Seas, enters the Argentine Basin in its southwest part and is redirected northwards, slowly sinking into deeper waters. If during its formation the AABW was also enriched in Hg, this could potentially explain the observed increase in THg. The process could be similar to the suggestion by *Fisher et al*. [2012] for the Arctic Ocean, where the melting of land ice with deposited Hg served as input to the Arctic waters or is the increase in THg due to higher wet Hg deposition [*Lamborg et al*., 2014]. Antarctic waters may also be enriched in Hg during their formation in the Weddell Sea where ice with deposited Hg melts and is incorporated into the Southern Ocean [*Cossa et al*., 2011; *Sonke and Heimbürger*, 2012].

Alternatively, the sediments may be locally important in this sedimentary basin, although they are thought to be globally negligible [*Mason et al*., 2012]. Hydrothermal sources are very unlikely because the Argentine Basin is geothermally inactive [*Hohertz and Carlson*, 1998]. The possibility exists that this observation may in fact be due to increased Hg(0) solubility at higher pressures [*Clever et al*., 1985]. The rapid sinking of cold water could help explain why deep waters of the AABW contain more DGM, compared to AAIW, which travels northward as surface water and only sinks at the Antarctic Convergence, thereby losing some of its original Hg content, which would explain the lower total estimation, compared to UCDW and NADW [*Thurman*, 1997]. It is also worth considering whether the onboard sampling process for DGM is likely to introduce an artefact or facilitate a false measurement. However, due to its high vapor pressure [*Barkay et al*., 2003] it is contraintuitive to imagine an *increase* in DGM values, and so a *decrease* (because of degassing) is much more probable.

DGM concentration in both basins was significantly different ($p < 0.05$), similar to Hg(0) values in North Atlantic, where western basin contained more Hg(0) than eastern [*Bowman et al*., 2015]. Unlike THg concentrations, which were more uniform, it appears that elemental Hg values remain different between the two basins in South Atlantic. At least 85% or more of DGM in water was in the form of Hg(0), considering the ratio DMeHg/DGM from Station 20, where DMeHg was determined. With respect to the life-time of Hg(0) in the water, this points to slow but constant processes, which continuously replenish Hg(0) in the water column and are in accord with chemical equilibrium of specific water mass. Whether these processes are microbial or geochemical or a combination thereof is difficult to gauge, however, if the conditions change, Hg speciation and fate will change also with respect to the type of prevalent reduction process.

In addition to interesting vertical strata of DGM in the South Atlantic Ocean, we have also observed an intriguing linear positive correlation of DGM with oxidized nitrogen species ($NO_3^- + NO_2^-$, further referred to only as nitrate, due to the comparatively low nitrite concentrations) ($R^2 = 0.75$, $p < 0.001$). Both DGM and nitrate values increase with depth, but their nutrient-like distribution can also be viewed as two larger cluster sample groups, one having low values near the surface and the other with higher values in the deep waters (Figure 7). The interest here is principally in the difference between the molecules; while DGM is actually an inert gas in the water, NO_3^- is an ion, forming hydrogen bonds with water molecules. Whether the observed correlation stems from a common biological process would need further investigation; however, these results

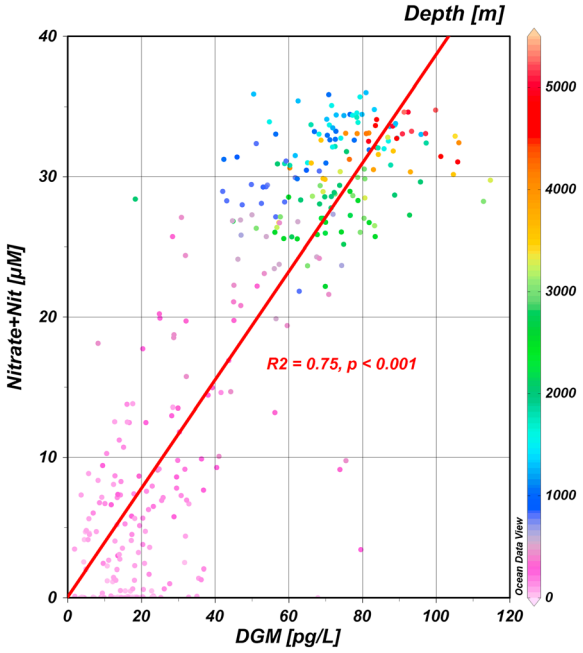

Figure 7. A positive correlation between sum of nitrate and nitrite with DGM. The correlation is very interesting ($R^2 = 0.75$, $p < 0.001$), because it indicates that other nutrients, apart from carbon cycle, may be involved to a certain level in Hg biogeotransformations. Furthermore, the figure shows the distribution of DGM in two broad groups: one associated with mixed layer and the other with deep ocean. Such decoupling between mixed layer and deep waters would mean that biogeotransformation processes differ in both realms and demonstrate that the Hg below mixed layer is removed from atmosphere for longer time periods.

are in accord with those of *Bowman et al.* [2015] and warrant more investigation. Nitrification and the nitrogen cycle in the deep ocean is almost entirely driven by microbial processes, but the extent of biological processes and chemical reactions, respectively, on Hg reduction in the deep ocean has not yet been sufficiently described [*Cossa et al.*, 2011; *Mason et al.*, 2012]. Nevertheless, there exists a theoretical possibility that nitrate reduction could be involved to some degree in DGM formation, because nitrification yields enough energy for Hg reduction. Furthermore, THg concentrations did not reach 10 ng/L, a threshold value for expression of *mer* operon; therefore, enzymatic Hg(0) production seems unlikely [*Barkay et al.*, 2003].

DGM and nitrate increase in the UCDW, which is on average lower in oxygen concentration [*Cossa et al.*, 2011]. Simultaneously, MeHg concentration seems to decrease slightly after UCDW, thus emphasizing connection of MeHg formation and OM degradation [*Heimbürger et al.*, 2010; *Cossa et al.*, 2011; *Lehnherr et al.*, 2011]. As a product of OM degradation, nitrate is released after its oxidation. Hence, in water masses with prolonged OM degradation, higher nitrate values are expected to coincide with higher MeHg values.However, it seems reasonable that energy, provided by microbial respiration, can be used either simultaneously or sequentially for either reduction and/or methylation of Hg(II). This spatiotemporal coupling would then be controlled by biotic activity and by the active fraction of the microbial community, shifting with respect to increasing recalcitrance of OM, shown to be degraded at different rates by various microbial genera [*Nagata et al.*, 2010].

The spatial separation of DGM values (lower near the surface and higher in deep waters; Figure 7) suggests that Hg biogeotransformations are conducted differently at both depths. Moreover, that would also suggest that Hg export from surface into the deep waters is not necessarily matched by an equal counterpart of upward transport and demonstrate that Hg in the intermediate waters and deep ocean is removed from atmospheric contact for considerably longer time periods [*Mason et al.*, 2012].

High nutrient, low chlorophyll (HNLC), and iron limited ACC surface waters that were observed during the cruise have, in general, shown less DGM and were dominated by larger cells of nanophytoplankton (e.g., some cyanobacteria and algae) [*Browning et al.*, 2014]. On the contrary, nutrient limited but not iron depleted water of the South Atlantic gyre was found to contain more smaller cells of picophytoplankton (*Prochlorococcus* and *Synechococcus*), but importantly, higher concentrations of DGM. This is not surprising, since oceanic phytoplankton blooms are often associated with enhanced Hg(0) production [*Rolfhus and Fitzgerald*, 2004]. *Marteyn et al.* [2013] have investigated the effect of a freshwater phototrophic microorganism *Synechocystis* PCC6803 on the reduction of Hg, emphasizing the lack of information relating to Hg reduction in nitrogen fixing photoautotrophs in general [*Grégoire and Poulain*, 2014]. In addition, presence of *mer* operon, responsible for enzymatic Hg reduction, has not been confirmed in phototrophic organisms [*Barkay et al.*, 2010; *Grégoire and Poulain*, 2014]. This could indicate that the DGM increase we observed was in fact due either to chemical reactions by secreted metabolites or was reduction conducted by associated heterotrophic community [*Grégoire and Poulain*, 2014].

4. Conclusions

The UK GEOTRACES South Atlantic Ocean cruise from South Africa to Uruguay along the 40°S parallel resulted in a high spatial (both vertical and horizontal) frequency of Hg speciation measurements. Up to 24 depths per station were measured, which proved to be sufficient to discern horizontal layering, although more samples would be preferable.

Unfortunately MeHg measurements were not as many as desired. Successful measurements usually correlated MeHg increase with lower oxygen concentration, substantiating that microbial respiration of organic matter stimulates MeHg formation. The general decrease at the surface might be indication of photo-demethylation. In two instances MeHg coincided with the chlorophyll *a* peak, which might relate MeHg formation with primary production, although this can also be a signal from the heterotrophic community, associated with photoautotrophs. The few positive measurements from above the sediment confirmed it as being a source of MeHg to the water column but also suggested that sediment is not an overall important contributor in this ocean region.

DMeHg was measured only at one station. As expected, it was higher in the intermediate and deep waters below 1000 m and very low above them, especially in the surface waters. It reached its highest concentration in the UCDW, similarly to DGM, probably due to lower oxygen concentrations and hence lower oxidation potential.

It appears that the western basin, in general, contains more Hg in all of its species. The mode of entry and natural/anthropogenic source could be illuminated by Hg stable isotope composition of end members. In addition, such investigation would evaluate the extent of Hg involvement in biogeochemical transformations which would be very valuable. THg values did not show much variation in the water column and were slightly higher on the western side of transect, possibly due to higher deposition. Surface waters always had lower THg concentrations compared to intermediate and deep, most likely due to evasion to the atmosphere. In deep waters, DGM represented as much as half of total THg. Overall, THg did not seem to be useful in tracing water masses.

The results show an interesting distribution of DGM. This oceanic region may be important as a global source of Hg^0 to the atmosphere. Besides bioreduction, photoreduction is also likely to occur in the uppermost layer. However, DGM formation and the presence of (photosynthetic) microorganisms were not always positively correlated in the photic zone, yet in the absence of any meaningful light influence or strong reducing agents in the deep ocean (aphotic zone), biotic reactions therefore appear to be primarily responsible for DGM formation. Surprisingly, water masses in the South Atlantic Ocean carry distinguishable DGM concentrations and further investigations and comparisons of different open ocean environments would be useful in determining possible usefulness of DGM as a geotracer. As a result of reducible Hg(II), DGM concentrations are useful hints to past and present Hg transformations in specific water masses, and to possible biogeochemical factors triggering the change in speciation.

Lastly, it is important to recognize that other nutrients may be directly or indirectly involved in microbially driven Hg ocean biotransformations. The already complex relationship between the Ocean and Hg may thus further emphasize the susceptibility of Hg cycle to global ocean change.

Acknowledgments

Data used in this paper are available at British Oceanographic Data Centre (doi: 10.5285/1dbc9294-4e65-6530-e053-6c86abc09fb2). The study was funded through NERC UK-GEOTRACES and Global Mercury Observation System (GMOS) projects (EU FP7) and through programme scheme P1-1043 and doctoral grant PR-03107 to A.B., both of Slovenian Research Agency (ARRS).The authors sincerely thank *RRS* James Cook crew and GA10 science crew for their selfless support and help, M. Pavlin, V. Fajon, M. Elskens for their much appreciated advice and assistance, and to G. M. Henderson for constructive comments and valuable review of the manuscript.

References

Amos, H. M., D. J. Jacob, D. Kocman, H. M. Horowitz, Y. Zhang, S. Dutkiewicz, M. Horvat, E. S. Corbitt, D. P. Krabbenhoft, and E. M. Sunderland (2014), Global biogeochemical implications of mercury discharges from rivers and sediment burial, *Environ. Sci. Technol.*, *48*, 9514–9522.

Azam, F., and F. Malfatti (2007), Microbial structuring of marine ecosystems, *Nat. Rev. Microbiol.*, *5*, 782–792.

Baldi, F. (1997), Microbial transformation of mercury species and their importance in the biogeochemical cycle of mercury, in *Metal Ions in Biological Systems, vol. 34: Mercury and its Effects on Environment and Biology*, edited by A. Sigel and H. D. Sigel, pp. 213–257, Dekker, New York-Basel-Hong Kong.

Barkay, T., and I. Wagner-Döbler (2005), Microbial transformations of mercury: Potentials, challenges, and achievements in controlling mercury toxicity in the environment, *Adv. Appl. Microbiol.*, *57*, 1–52.

Barkay, T., M. Gillman, and R. R. Turner (1997), Effects of dissolved organic carbon and salinity on bioavailability of mercury, *Appl. Environ. Microbiol.*, *63*, 4267–4271.

Barkay, T., S. M. Miller, and A. O. Summers (2003), Bacterial mercury resistance from atoms to ecosystems, *FEMS Microbiol. Rev.*, *27*, 355–384.

Barkay, T., K. Kritee, E. Boyd, and G. Geesey (2010), A thermophilic bacterial origin and subsequent constraints by redox, light and salinity on the evolution of the microbial mercuric reductase, *Environ. Microbiol.*, *12*, 2904–2917.

Bloom, N. S., and W. F. Fitzgerald (1988), Determination of volatile mercury species at the picogram level by low temperature gas chromatography with cold-vapour atomic fluorescence detector, *Anal. Chim. Acta*, *208*, 151–161.

Bowman, K. L., C. R. Hammerschmidt, C. H. Lamborg, and G. Swarr (2015), Mercury in the North Atlantic OCean: The U.S. GEOTRACES zonal and meridional sections, *Deep Sea Res.*, Part II, *116*, 251–261, doi:10.1016/j.dsr2.2014.07.004.

Bratkič, A., N. Ogrinc, J. Kotnik, J. Faganeli, D. Žagar, S. Yano, A. Tada, and M. Horvat (2013), Mercury speciation driven by seasonal changes in a contaminated estuarine environment, *Environ. Res.*, *125*, 103–112.

Browning, T. J., H. A. Bouman, C. M. Moore, C. Schlosser, G. A. Tarran, E. M. S. Woodward, and G. M. Henderson (2014), Nutrient regimes control phytoplankton ecophysiology in the South Atlantic, *Biogeosciences*, *11*, 463–479.

Clever, H. L., S. A. Johnson, and E. M. Derrick (1985), The solubility of mercury and some sparingly soluble mercury salts in water and aqueous electrolyte solutions, *J. Phys. Chem. Ref. Data*, *14*, 631–680.

Coquery, M., and D. Cossa (1995), Mercury speciation in surface waters of the north sea, *Neth. J. Sea Res.*, *34*, 245–257.

Cossa, D., M. H. Cotte–Krief, R. P. Mason, and J. Bretaudeau–Sanjuan (2004), Total mercury in the water column near the shelf edge of the european continental margin, *Mar. Chem.*, *90*, 21–29.

Cossa, D., L.-E. Heimbürger, D. Lannuzel, S. R. Rintoul, E. C. V. Butler, A. R. Bowie, B. Averty, R. J. Watson, and T. Remenyi (2011), Mercury in Southern Ocean, *Geochim. Cosmochim. Acta*, *75*, 4037–4052.

Donners, J., S. S. Drijfhout, and W. Hazeleger (2005), Water mass transformation and subduction in the South Atlantic, *Am. Meteorol. Soc.*, *35*, 1841–1860.

Emery, W. J. (2001), Water types and water masses, in *Encyclopedia of Ocean Sciences*, edited by J. Steele, S. Thrope, and K. Turekain, pp. 3179–3187, Academic Press.

Emili, A., N. Koron, S. Covelli, J. Faganeli, A. Acquavita, S. Predonzani, and C. De Vittor (2011), Does anoxia affect mercury cycling at the sediment-water interface in the Gulf of Trieste (northern Adriatic Sea)? Incubation experiments using benthic flux chambers, *Appl. Geochem.*, *26*, 194–204.

Fisher, J. A., D. J. Jacob, A. Soerensen, H. M. Amos, A. Steffen, and E. M. Sunderland (2012), Major river sources of Arctic Ocean mercury inferred from atmospheric observations, *Nat. Geosci.*, *4*, 499–504.

Fitzgerald, W. F., and C. H. Lamborg (2003), Geochemistry of mercury in the environment, in *Treatise on Geochemistry*, vol. 9, chap. 4, pp. 107–148, Elsevier, Amsterdam.

Fitzgerald, W. F., C. H. Lamborg, and C. R. Hammerschmidt (2007), Marine biogeochemical cycling of mercury, *Chem. Rev.*, *107*, 641–662.

Gårdfeldt, K., J. Sommar, R. Ferrara, C. Ceccarini, E. Lanzillotta, V. Fajon, F. Sprovieri, N. Pirrone, and I. Wangberg (2003), Evasion of mercury from coastal and open waters of the Atlantic Ocean and the Mediterranean Sea, *Atmos. Environ.*, *37*, S73–S84.

Grégoire, D. S., and A. J. Poulain (2014), A little bit of light goes a long way: The role of phototrophs on mercury cycling, *Metallomics*, *6*, 396–407.

Hammerschmidt, C. R., and K. L. Bowman (2012), Vertical methylmercury distribution in the subtropical North Pacific Ocean, *Mar. Chem.*, *132–133*, 77–82.

Heimbürger, L.-E., D. Cossa, J.-C. Marty, C. Migon, B. Averty, A. Dufour, and J. Ras (2010), Methyl mercury distributions in relation to the presence of nano- and picophytoplankton in an oceanic water column (Ligurian Sea, North-Western Mediterranean), *Geochim. Cosmochim. Acta*, *74*, 5549–5559.

Herndl, G. J., and T. Rheinthaler (2013), Microbial control of the dark end of the biological pump, *Nat. Geosci.*, *6*, 718–724.

Hines, M. E., J. Faganeli, I. Adatto, and M. Horvat (2006), Microbial mercury transformations in marine, estuarine and freshwater sediment downstream of the Idrija Mercury mine Slovenia, *Appl. Geochem.*, *21*, 1924–1939.

Hohertz, W. L., and R. L. Carlson (1998), An independent test of thermal subsidence and asthenosphere flow beneath the Argentine Basin, *Earth Planet. Sci. Lett.*, *161*, 73–83.

Horvat, M., L. Liang, and N. S. Bloom (1993), Comparison of distillation with other current isolation methods for the determination of methyl mercury compounds in low level environmental samples: Part II: Water, *Anal. Chim. Acta*, *282*, 153–168.

Horvat, M., J. Kotnik, M. Logar, V. Fajon, T. Zvonarić, and N. Pirrone (2003), Speciation of mercury in surface and deep-sea waters in the Mediterranean Sea, *Atmos. Environ.*, *37*(1), S93–S108.

Hydes, D. J., et al. (2010), Determination of dissolved nutrients (N, P, Si) in seawater with high precision and inter-comparability using gas-segmented continuous flow analysers, *The GO-SHIP Repeat Hydrography Manual*: *A Collection of Expert Reports and Guidelines*; *IOCCP Rep. 14*, ICPO Publication Series 134, Version 1.

Johnson, M. S., N. Meskhidze, V. P. Kiliyanpilakkil, and S. Gassó (2011), Understanding the transport of Patagonian dust and its influence on marine biological activity in the South Atlantic Ocean, *Atmos. Chem. Phys.*, *11*, 2487–2502.

Kocman, D., M. Horvat, N. Pirrone, and S. Cinnirella (2013), Contribution of contaminated sites to the global mercury budget, *Environ. Res.*, *125*, 160–170.

Kotnik, J., et al. (2007), Mercury speciation in surface and deep waters of the Mediterranean Sea, *Mar. Chem.*, *107*, 13–30.

Lamborg, C. H., K. L. Von Damm, W. F. Fitzgerald, C. R. Hammerschmidt, and R. Zierenberg (2006), Mercury and monomethylmercury in fluids from Sea Cliff submarine hydrothermal field, Gorda Ridge, *Geophys. Res. Lett.*, *33*, L17606, doi:10.1029/2006GL026321.

Lamborg, C. H., C. R. Hammerschmidt, K. L. Bowman, G. J. Swarr, K. M. Munson, D. C. Ohnemus, P. J. Lam, L.-E. Heimbürger, M. J. A. Rijkenberg, and M. A. Saito (2014), A global ocean inventory of anthropogenic mercury based on water column measurements, *Nature*, *512*, 65–68.

Lehnherr, I., V. L. S. Louis, H. Hintelmann, and J. L. Kirk (2011), Methylation of inorganic mercury in polar marine waters, *Nat. Geosci.*, *4*, 298–302.

Leopold, K., M. Foulkes, and P. Worsfold (2010), Methods for determination and speciation of mercury in natural waters – a review, *Anal. Chim. Acta*, *663*, 127–138.

Liang, L., M. Horvat, and N. S. Bloom (1994), An improved method for speciation of mercury by aqueous phase ethylation, room temperature precollection GC separation and CV AFS detection, *Talanta*, *41*, 371–379.

Marteyn, B., S. Sakr, S. Farci, M. Bedhomme, S. Chardonnet, P. Decottignies, S. D. Lemaire, C. Cassier-Chauvat, and F. Chauvat (2013), The synechocystis PCC6803 MerA-like enzyme operates in the reduction of both mercury and uranium under the control of the glutaredoxin 1 enzyme, *J. Bacteriol.*, *195*, 4138–4145.

Mason, R. P., and K. A. Sullivan (1999), The distribution and speciation of mercury in the South and equatorial Atlantic, *Deep Sea Res., Part II*, *46*, 937–956.

Mason, R. P., K. R. Rolfhus, and W. F. Fitzgerald (1998), Mercury in the North Atlantic, *Mar. Chem.*, *61*, 37–53.

Mason, R. P., E.-H. Kim, J. Cornwell, and D. Heyes (2006), An examination of the factors influencing the flux of mercury, methylmercury and other constituents from estuarine sediment, *Mar. Chem.*, *102*, 96–110.

Mason, R. P., A. L. Choi, W. F. Fitzgerald, C. R. Hammerschmidt, C. H. Lamborg, A. K. Soerensen, and E. M. Sunderland (2012), Mercury biogeochemical cycling in the ocean and policy implications, *Environ. Res.*, *119*, 101–117.

Merritt, K. A., and A. Amirbahman (2009), Mercury methylation dynamics in estuarine and coastal marine environments – a critical review, *Earth Sci. Rev.*, *96*, 54–66.

Monperrus, M., E. Tessier, D. Amouroux, A. Leynaert, P. Huonnic, and O. F. X. Donard (2007), Mercury methylation, demethylation and reduction rates in coastal and marine surface waters of the Mediterranean Sea, *Mar. Chem.*, *107*, 49–63.

Nagata, T., et al. (2010), Emerging concept son microbial processes in the bathypelagic ocean – ecology, biogeochemistry, and genomics, *Deep Sea Res., Part II*, *57*, 1519–1536.

Ogrinc, N., M. Monperrus, J. Kotnik, V. Fajon, K. Vidimova, D. Amouroux, D. Kocman, E. Tessier, S. Žižek, and M. Horvat (2007), Distribution of mercury and methylmercury in deep-sea surficial sediments of the Mediterranean Sea, *Mar. Chem.*, *107*, 31–48.

Pirrone, N., et al. (2010), Global mercury emissions to the atmosphere from anthropogenic and natural sources, *Atmos. Chem. Phys.*, *10*, 5951–5964.

Pongratz, R., and K. G. Heumann (1998), Production of methylated mercury by polar microalgae – A significant natural source for atmospheric heavy metals in clean room compartments, *Chemosphere*, *36*, 1935–1946.

Rolfhus, K. R., and W. F. Fitzgerald (2004), Mechanisms and temporal variability of dissolved gaseous mercury production in coastal seawater, *Mar. Chem.*, *90*, 125–136.

Ronco, A. E., M. C. Camilión, and M. J. Manassero (2001), Geochemistry of heavy metals in bottom sediments from streams of the western coast of the Río de la Plata estuary Argentina, *Environ. Geochem. Health*, *23*, 89–103.

Sonke, J. E., and L.-E. Heimbürger (2012), Environmental science: Mercury in flux, *Nat. Geosci.*, *5*, 447–448.

Sunderland, E. M., D. P. Krabbenhoft, J. W. Moreau, S. A. Strode, and W. M. Landing (2009), Mercury sources, distribution, and bioavailability in the North Pacific Ocean: Insights from data and models, *Global Biogeochem. Cycles*, *23*, GB2010, doi:10.1029/2008GB003425.

Thurman, H. V. (1997), *Introductory Oceanography*, 8th ed., Prentice Hall, Upper Saddle River, N. J.

Tomczak, M., and J. S. Godfrey (1994), Hydrology of the Atlantic Ocean, in *Regional Oceanography: An Introduction*, edited by M. Tomczak and J. S. Godfrey, pp. 253–270, Elsevier, New York.

United Nations Environment Programme (UNEP) (2013), *Global Mercury Assessment 2013: Sources, Emissions, Releases and Environmental Transport*, UNEP Chemicals Branch,
Geneva, Switzerland.

Vetriani, C., Y. S. Chew, S. M. Miller, J. Yagi, J. Coombs, R. A. Lutz, and T. Barkay (2005), Mercury adaptation among bacteria from a deep-sea hydrothermal vent, *Appl. Environ. Microbiol.*, *71*, 220–226.

Woodward, E. M. S., and A. P. Rees (2001), Nutrient distributions in an anticyclonic eddy in the North East Atlantic Ocean, with reference to nanomolar ammonium concentrations, *Deep Sea Res.*, *48*, 775–794.

Wyatt, N. J., A. Milne, E. M. S. Woodward, A. P. Rees, T. J. Browning, H. A. Bouman, P. J. Worsfold, and M. C. Lohan (2014), Biogeochemical cycling of dissolved zinc along the GEOTRACES South Atlantic transect GA10 at 40°S, *Global Biogeochem. Cycles*, *28*, 44–56, doi:10.1002/2013GB004637.

Zhang, Y., L. Jaeglé, and L. A. Thompson (2014), Natural biogeochemical cycle of mercury in a global three-dimensional ocean tracer model, *Global Biochem. Cycles*, *28*, 553–570, doi:10.1002/2014GB004814.